



Study on Mechanical Properties, Microstructure and Corrosion Behaviour of Cu-10Ni Alloy with Varying La Contents and Ageing Parameters

Augustine B. Okoubulu¹ and Cynthia C. Nwaeju-Okechukwu^{2,3*}

¹Department Materials and Metallurgical Engineering, Southern Delta University, P.M.B. 5, Ozoro, Nigeria

²Department of Mechanical Engineering, Nigeria Maritime University, Okerenkoko, Delta State, Nigeria

³Department of Metallurgical and Materials Engineering, Nnamdi Azikiwe University, P.M.B. 5025 Awka, Nigeria

Abstract

This study investigates the influence of lanthanum (La) microalloying and ageing treatment on the microstructural evolution, mechanical performance, and corrosion behaviour of Cu-10Ni alloys. Alloys containing 0, 0.1, 0.2, 0.3, and 1.5 wt.% La were prepared through an optimization process and aged at temperatures of 400, 450, and 500 °C for a constant duration of 4 hours. Characterization was then carried out using optical microscopy (OM), scanning electron microscopy (SEM), mechanical testing, and electrochemical polarization analysis. The results reveal that low-to-moderate La additions (0.1-0.3 wt.%) significantly refine the grain structure, purify grain boundaries, and promote the formation of uniformly distributed nanoscale La-rich precipitates. These microstructural modifications lead to substantial improvements in tensile strength, hardness, toughness, and corrosion resistance. The alloy containing 0.3 wt.% La aged at 450 °C exhibited the most favourable balance of properties, achieving a tensile strength of 542 MPa, hardness of 166.1 HBW, toughness of 78 J, and the lowest corrosion current density. Strengthening was governed by a synergistic combination of grain refinement, precipitation hardening, and Orowan looping. In contrast, excessive La addition (1.5 wt.%) and over-ageing at 500 °C resulted in precipitate coarsening, semi-continuous grain boundary phases, and degraded mechanical and electrochemical performance. Optimization results confirmed that Cu-10Ni-0.2La aged at 450 °C gives the most favourable balance of strength, toughness and corrosion resistance, whereas higher La levels yield limited strength gains but reduced overall performance. The combined experimental and ANFIS optimization findings demonstrate that controlled La microalloying in the range of 0.2 - 0.3 wt.% combined with ageing at is 450 °C gives the most favourable compromise between strength, toughness and corrosion resistance.

Paper type: Research Paper

Keywords: Cu-Ni-xLa alloy, Ageing temperature, mechanical properties, Grain refinement, Corrosion behaviour.

Citation: Okoubulu, A. B., and Nwaeju-Okechukwu, C.C., " Study on Mechanical Properties, Microstructures and Corrosion Resistance of Cu-10Ni Alloy with Varying La Contents and Ageing Parameters" *Jordanian Journal of Engineering and Chemical Industries*, Vol. 9, No.1, pp:63-76 (2026).

1. Introduction

Copper-nickel alloys (Cu-Ni) play an important role in modern engineering, particularly in thermal, marine, and power generation systems. Their excellent resistance to seawater corrosion, good thermal stability, and moderate mechanical strength make them suitable for condenser tubes, pump components, and piping in power plants (Guo et al, 2021; Nwaeju et al., 2021). However, as the demands on operating environments increase, particularly at high temperatures or in areas of severe corrosion, the traditional Cu-10Ni alloy is increasingly reaching its limits due to its relatively low strength and moderate age-hardening response. These limitations restrict its use in applications requiring higher mechanical properties and a longer service life (Semboshi et al., 2021; Hou et al., 2021). To improve

* Corresponding author: E-mail: cynthianwaeju@gmail.com
Received: 28/January/2026

ORCID: 0000-0001-6796-3651
Revised: 09/March/2026



the strength of Cu-Ni alloys, several researchers have investigated precipitation hardening through small additions of alloying elements such as Si, Cr, or Fe in combination with thermomechanical treatments. For example, Cu-Ni-Si alloys benefit from the formation of Ni₂Si precipitates, which significantly increase hardness and strength while maintaining ductility (Krupińska et al., 2020). Although these strategies offer useful improvements, they often require higher alloy contents or complex processing steps. In many cases, they can also compromise corrosion resistance, particularly in chloride-rich marine environments (Peng et al., 2023).

Microalloying with rare earth elements (RE) has recently established itself as an attractive alternative for improving copper alloys. Even at very low concentrations, Rare elements can refine the grain structure, purify melts by removing oxygen and sulphur, stabilize grain boundaries, and promote the formation of fine dispersoids that hinder dislocation movement (Liu et al., 2025; Yu et al., 2025). Lanthanum (La) has proven to be a promising microstructure regulator in steels, aluminium alloys, and various copper alloys. These effects collectively improve strength, thermal stability, and often corrosion resistance. Despite this potential, however, few studies have investigated the effects of La on Cu-Ni alloys. Existing work on La in Cu-Ni-Si or Cu-Al-Ni alloys shows encouraging improvements but does not directly address the Cu-Ni system, resulting in a significant knowledge gap. For example, Aliyu et al. (2024) investigated La additions in Cu Al-Ni alloys and reported grain refinement and improved mechanical properties, but they did not address the Cu Ni system. Wang et al. (2023) also examined the La effects in Cu Ni-Si alloys and demonstrated increased thermal stability and hardness. However, they emphasized the lack of systematic data on La concentration and heat treatment interactions during in Cu Ni alloys. Further studies on rare earth elements in Al Si-Cu alloys (Mahmoud et al., 2021) and steels (Ji et al., 2018; Liu et al., 2023) confirm the general role of rare earth elements as grain refiners and impurity scavengers, but do not provide detailed insights into Cu Ni alloys. In particular, the combined influence of La concentration and ageing temperature on the microstructure development, strength, ductility, and toughness of Cu-Ni alloys is still insufficiently understood. This lack of data hinders the development of design guidelines for next-generation Cu-Ni materials that must function reliably in corrosive and thermally demanding environments such as desalination plants, ship cooling systems, offshore installations, and high-temperature condensers.

This study addresses this research gap by developing and evaluating lanthanum microalloying (0-1.5 wt%) in Cu-Ni alloys combined with ageing parameters, supported by ANFIS optimization. Using controlled melting, homogenization, solution treatment, and aging at 400-500 °C, we investigate the influence of lanthanum additions on grain refinement, precipitation formation, mechanical behaviour, impact toughness, and corrosion resistance.

2. Materials and Methods

2.1 Materials and Alloy design

The materials used in the experiment include electrolytic copper (99.9%), nickel (99.96%), and high-purity lanthanum (99.5%). The lanthanum which belongs to the family of rare earth metals is used as the refining agent. The electrolytic copper wire and nickel granules were used as the base materials. These materials were procured from Cifa laboratories (CIBIS) New Heaven Enugu, and Cutis Cable Plc Nnewi, Nigeria. The materials were weighed according to the calculated proportions. Alloy Composition Design: Five composition formulation of Cu-10 wt% Ni alloys were prepared with varying trace additions of lanthanum (La) at concentrations of 0, 0.1, 0.2, 0.3, and 1.5 wt% to establish a composition-property profile for low to moderate rare-earth microalloy grades.

2.2 Alloy Fabrication

The melting and casting process were carried out in a high-frequency crucible furnace under an argon atmosphere to minimize oxidation (Yu et al., 2025; Liu et al., 2025). The fabrication process was carefully controlled to ensure consistency and homogeneity. First, pure copper was melted under a protective atmosphere at about 1085°C under a protective atmosphere of argon. Once fully molten at about 1200 °C, the alloying elements (Ni and La) were gradually added to the melt. To ensure even distribution, the mixture was mechanically stirred. The mixture was stirred for 10 min at 200 rpm to achieve uniform dispersion. The homogenized melt was then poured into a preheated permanent steel mould (10044 EU grade), heated to 100 °C, with internal dimensions of 70 mm diameter, 220 mm height and 5 mm wall thickness.

To further improve the casting quality, the filled mould was transferred to a tube furnace and held for 5 minutes at 670 °C under the same protective gas atmosphere. This step facilitated the settling of the inclusions. The mould was then lowered into the cooling chamber, with water supplied at a controlled rate of 10 mm/s to solidify the alloy under near-ideal conditions. Similar casting processes for Cu-Ni-RE alloys have been reported in recent studies (Wang et al, 2023; Zhang et al, 2024). The chemical composition of the resulting alloys was precisely characterized using spark emission spectrometry (Spectrolab M9, Ametek-Spectro, Kleve, Germany) and the result is listed in **Table 1**.

Table 1: Specific Compositions of the Experimental Alloys (wt%)

Alloys	Ni (wt%)	Si (wt%)	Zn (wt%)	La (wt.%)	Fe (wt%)	Cu (wt%)
Cu-10Ni	9.98	0.0056	0.0028	0.00	0.0046	balance
Cu-10Ni-0.1La	9.97	0.0053	0.0022	0.11	0.0039	balance
Cu-10Ni-0.2La	10.00	0.0050	0.0020	0.19	0.0043	balance
Cu-10Ni-0.3La	9.90	0.0052	0.0022	0.28	0.0037	balance
Cu-10Ni-1.5La	9.98	0.0046	0.0019	1.49	0.0038	balance

2.3 Thermal Treatment

After surface defects from the casting were removed, the casting ingots obtained were homogenized at 920 °C for 5 hours and then cooled in air at ambient temperature. This process was to prevent dendrite formation and segregation during the casting process (Shi et al., 2023). The samples were also solution-treated at 800 °C for 2 hours and quenched in cold water to obtain a supersaturated solid solution. Solutionizing + quenching is the standard way to enable precipitation hardening (Zhou et al, 2024). To investigate the influence of thermal exposure on precipitation behaviour and matrix stabilization, samples of different compositions were aged for 4 hours at 400 °C, 450 °C, and 500 °C and subsequently cooled in air. These parameters were selected based on previous studies demonstrating their effectiveness in improving precipitation hardening and grain boundary stabilization in copper alloys (Zhou et al., 2024). Special attention was given to the Cu-10Ni-0.2La alloy aged at 450 °C, which, through ANFIS optimization, was identified as the prime candidate for a balanced ratio of strength, ductility, corrosion resistance, and thermal stability. Comparison alloys were aged at the following temperatures: 0.1 wt.% La at 400 °C, 0.3 wt.% La at 450 °C and 500 °C, and 1.5 wt.% La at 400 °C (to assess dispersoid stabilization at moderate temperatures).

2.3.1 ANFIS Optimization Methodology

To further support the experimental results, an Adaptive Neuro-Fuzzy Inference System (ANFIS) model was used to optimize the relationship between lanthanum content, ageing temperature and the resulting mechanical and corrosion properties of the Cu-10Ni-xLa alloys. The aim of this model was to identify the alloy composition, thermal treatment parameters that give the best overall performance by maximizing strength, toughness and resistance to corrosion (Nwaeju-Okechukwu et al., 2025). The model design layout is presented in **Table 2**.

Input Parameters

The model considered two main input variables:

- Lanthanum content (wt.%): 0, 0.1, 0.2, 0.3, and 1.5
- Ageing temperature (°C): 400, 450 and 500

Output Parameters

The selected outputs were the critical performance criteria used to evaluate the alloys:

- Ultimate tensile strength (MPa)
- Hardness (HBW)
- Impact toughness (J)
- Corrosion current density ($\mu\text{A}/\text{cm}^2$)

Table 2. ANFIS Model Structure Summary

Parameter	Description
FIS Type	Sugeno-type
Number of Inputs	2
Number of Outputs	4
Membership Function	Gaussian

MFs per Input	3
Total Fuzzy Rules	9
Training Algorithm	Hybrid (LSE + Backpropagation)
Training Epochs	100
Error Tolerance	1×10^{-4}

2.4 Characterization Method

For comprehensive microstructural analysis, samples of each alloy composition were carefully prepared for optical microscopy (OM). The samples were embedded in a cold-curing plastic resin and sequentially ground with SiC abrasive paper up to a grit size of 2400. They were then polished with a suspension of 1 μm diamond particles, followed by final polishing with 0.05 μm colloidal silica to achieve a mirror-like surface. The polished surfaces were then etched in a 30% $\text{FeCl}_3\text{-HCl}$ solution. Metallurgical microstructure analysis was performed using an optical microscope (OM, Axio Observer A1 Zeiss, Carl Zeiss AG, Oberkochen, Germany). Scanning electron microscopy (SEM) was performed using a Zeiss Sigma SEM, which is equipped for high-resolution imaging of intermetallic phases, grain boundaries, and precipitate distributions. These techniques enabled the quantitative determination of grain size development, precipitation morphology, and the formation of La-rich dispersoids. The mechanical properties were established by assessing the UTS, ductility, hardness, and impact energy. Hardness was measured on a Brinell hardness tester (model 900-355). Several measurements were conducted to achieve statistical reliability. Tensile testing was also carried out with an Instron universal testing machine (model 3369), at a strain rate of 10^{-3} s^{-1} , according to the ASTM B557M standard. Impact toughness was measured by using standard Charpy V-notch specimens ($55 \times 10 \times 10 \text{ mm}^3$, 2 mm V-notch depth, 45° notch angle, and 0.25 mm notch tip radius) according to ASTM E23. The specimens were cut from heat-treated samples. Tests were conducted at $23 \pm 2^\circ \text{C}$ by using a pendulum impact tester (model U1820) with a capacity of 300 J. Three specimens for each alloy and heat-treatment condition were tested ($n = 3$), and the average impact energy (J) with the standard deviation was presented. All mechanical properties were calculated as the average of at least three specimens. The corrosion resistance properties were tested using potentiodynamic polarization techniques in a neutral environment containing 3.5 wt% NaCl, which resembles seawater, using an Autolab CH1604E electrochemical system. A three-electrode arrangement was adopted, which included a saturated calomel electrode (SCE), platinum plate, and alloy sample with an exposed area of 1 cm^2 acting as the working electrode. The samples ($3.0 \times 1.0 \times 0.2 \text{ cm}$) were successively ground with abrasive paper (grit 200-1000), rinsed with distilled water, degreased with acetone, and embedded in epoxy resin. A 3.5 wt% NaCl solution at 25°C , simulating seawater, served as the corrosion medium. The open-circuit potential (OCP) was recorded for 3000 s to achieve stabilization. Subsequently, electrochemical impedance spectroscopy (EIS) in the frequency range of 100 kHz to 5 mHz ($\pm 5 \text{ mV}$ amplitude) and potentiodynamic polarization measurements were performed to determine the corrosion current density and rate.

3. Results and Discussion

3.1 Chemical Composition and Casting Quality

The results of the spark OES analysis (**Table 1**) confirmed that all alloys largely achieved the target compositions. The Ni content ranged from 9.90 to 10.00 wt.%, and the La additions were within the target range of 0 to 1.5 wt.%. The low levels of impurities ($\text{Fe} < 0.005 \text{ wt.}\%$; $\text{Si} < 0.006 \text{ wt.}\%$; $\text{Zn} < 0.003 \text{ wt.}\%$) confirm the successful control of melt impurities during casting. This high degree of compositional accuracy is essential, as traces of rare earth metals are highly susceptible to oxidation during melting and are lost (Zhang et al., 2024). Inductive melting under an argon atmosphere and subsequent settling in the mould at 670°C contributed to the visibly pure microstructures of all alloys. Water-assisted, controlled cooling (10 mm/s) effectively suppressed hot tearing and macrosegregation. Similar results were reported for Cu-Ni-RE alloys by Wang et al. (2023), who observed that controlled post-fill heat holding promotes inclusions flotation, especially La-rich oxides/sulphides.

3.2 Mechanical Properties

The mechanical properties of the investigated Cu-10Ni-xLa alloys ($x = 0, 0.1, 0.2, 0.3, \text{ and } 1.5 \text{ wt.}\%$) are summarized in **Figures 1, 2 and 3**. With the progressive addition of La and subsequent ageing heat treatment, significant improvements in tensile strength, hardness, and impact strength were observed.

3.2.1 Tensile Properties

Figure 1 shows the variations of ultimate tensile strength (UTS) and elongation percentage of the alloys prepared at the ageing temperature of 400 °C, 450 °C, and 500 °C. At all ageing treatments, the Cu-10Ni-xLa alloys showed better mechanical properties than the base Cu-10Ni alloy. The UTS of the base Cu-10Ni alloy increased markedly from 305 MPa to a maximum of 542 MPa following trace lanthanum addition and subsequent ageing heat treatment. The strengthening effect was most pronounced in the La content range of 0.2–0.3 wt.%. The Cu-10Ni-0.1La alloy aged under 400 °C conditions resulted in a UTS value of 485 MPa, whereas for the Cu-10Ni-0.2La alloy, there was an improvement in UTS value to 520 MPa for aging conditions of 450°C. The highest value of UTS was found to be for Cu-10Ni-0.3La alloy aged under 450 °C conditions to 542 MPa. Such observations in terms of strength improvement can easily be explained in terms of the metallurgical requirements of lanthanum addition in Cu-Ni alloys. La has affinity for oxygen, sulphur, and grain boundary impurities; as such, it has been found to have micro-cleaning and grain refinement properties (Liu et al. 2023; Aliyu et al. 2024; Lian et al. 2022). In addition, La promotes the formation of thermally stable, nanoscale La-rich precipitates that impede dislocation motion and pin grain boundaries, resulting in enhanced precipitation hardening (Zhang et al., 2024; Wang et al., 2024). The slight decrease in UTS in the alloy containing 0.3 wt.% of La aged at 500 °C (493 MPa) reflects an over-aged state where precipitates lose their effectiveness in material hardening due to coarsening (Semboshi et al., 2021; Wu et al., 2025). Likewise, ductility (viz., % elongation) was significantly higher from 12.4% (0 wt.% La) to 24.05% (0.3 wt.% La at 500 °C). Generally, solute species, precipitation-hardening precipitates, and dispersoids are regarded as the principal strengthening components of copper alloys (Wang et al., 2023).

A clear inverse relationship between strength and ductility was seen across the alloys: elongation at break in the control alloy (12.4%) steadily increased with increase in La content up to 24.05% in the alloy doped with 0.3 wt.% of La. The reason behind this is related to the uniform dispersion of second-phase particles in the microstructures which resist dislocation strengthening but increase ductility (Zhang et al., 2024).

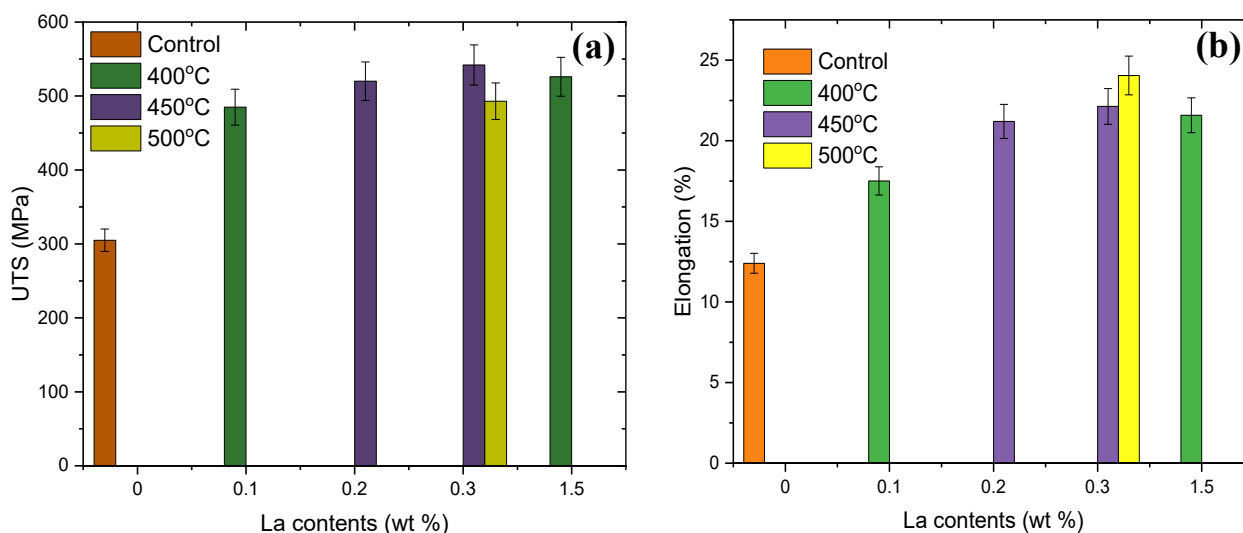


Fig. 1. Tensile properties of Cu-10Ni-xLa alloys at different ageing temperature: (a) Ultimate tensile strength and (b) Percentage elongation (ductility).

3.2.2 Hardness Evolution

The hardness of the developed Cu-10Ni-xLa alloys at different ageing temperatures is presented in Fig. 2. As shown in Fig. 2, the evolution of hardness closely mirrors the tensile behaviour of the alloys. This trend can be attributed to the combined effects of solid-solution strengthening and work hardening induced by the addition of the rare-earth element La.

With addition of La at different concentration, the hardness of the alloys generally increased combined with the ageing process. From the plotted chart (Fig 2), it could be observed that the as-cast Cu-10Ni alloy (the base alloy) exhibited the lowest hardness value of 115.3 HBW, which increased progressively with La additions up to 1.5 wt.%. The optimum hardness of 166 HBW was achieved for the Cu-10Ni-0.3La alloy aged at 450 °C. Notably, significant hardness enhancement was observed in the alloy with with micro-additions of La after the heat treatment. The macro-addition of La at moderate ageing temperature (400 °C) accelerate precipitate

formation, thereby enhancing the hardening rate. Hence, the reduction in hardness observed for the 0.3 wt.% La alloy aged at 500 °C can be attributed to over-ageing effects. As reported by Jing et al. (2026), post peak ageing, -induced softening which always becomes dominant, causing hardness to decrease more rapidly at elevated temperature. Precipitation ageing enhances strength while suppressing the work-hardening rate due to the formation of nanoscale β''/β' precipitates uniformly dispersed within the alloy matrix (Cuniberti et al., 2010). This result is consistent with the trends reported in rare-earth-modified copper alloys, where excessive rare-earth additions promote the formation of coarse, brittle intermetallic compounds that adversely affect hardness (Wang et al., 2023; Aliyu et al., 2024).

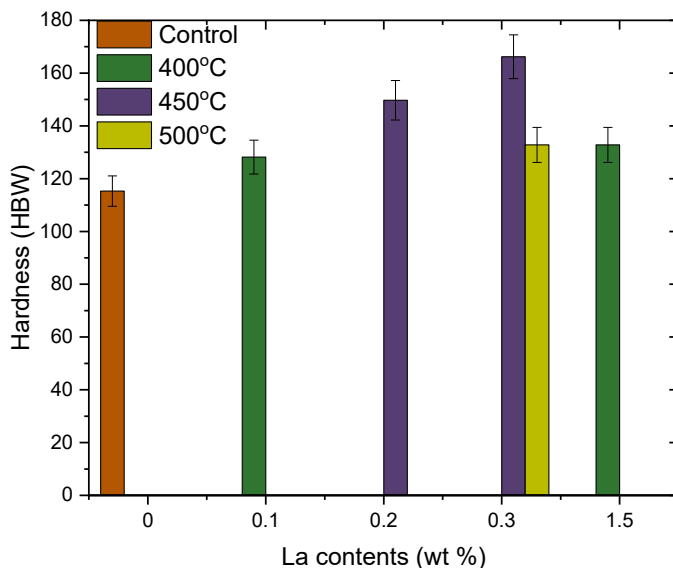


Fig. 2. Hardness of Cu-10Ni-xLa alloys at different ageing temperatures.

3.2.3 Impact Energy

The impact energy results of the Cu-10Ni-xLa alloys after ageing are presented in Fig 3. The base Cu-10Ni alloy exhibited the lowest impact energy of 60 J, indicating limited resistance to crack initiation and propagation. With the addition of lanthanum and subsequent ageing treatment, a marked improvement in impact toughness was observed. Micro-additions of La significantly enhanced the impact energy, with the Cu-10Ni-0.1La alloy aged at 400 °C recording the highest value of 86 J. This improvement can be attributed to grain refinement and effective impurity scavenging by La, which reduces stress concentration sites and promote more uniform plastic deformation during impact loading. Further increases in La content to 0.2 and 0.3 wt.% resulted in slightly reduced impact energies (80 J and 78 J, respectively), despite continued increases in strength and hardness. This behaviour reflects the typical strength-toughness trade-off, where enhanced precipitation strengthening and increased dislocation density restrict plastic deformation and limit energy absorption during fracture. At higher La content and elevated ageing temperature, the impact energy decreased further, as observed for the Cu-10Ni-0.3La alloy aged at 500 °C (77 J). This reduction is associated with over-ageing effects and precipitate coarsening, which promote localised brittle fracture and reduce crack blunting capability. Similar trends have been reported in rare-earth-modified copper alloys, where excessive rare-earth additions lead to the formation of coarse intermetallic phases that degrade toughness, despite improving strength (Wang et al., 2023; Aliyu et al., 2024; Nwaeju et al., 2022). Overall, the results indicate that controlled micro-additions of La combined with appropriate ageing conditions provide an optimal balance between strength and impact toughness in Cu-10Ni alloys.

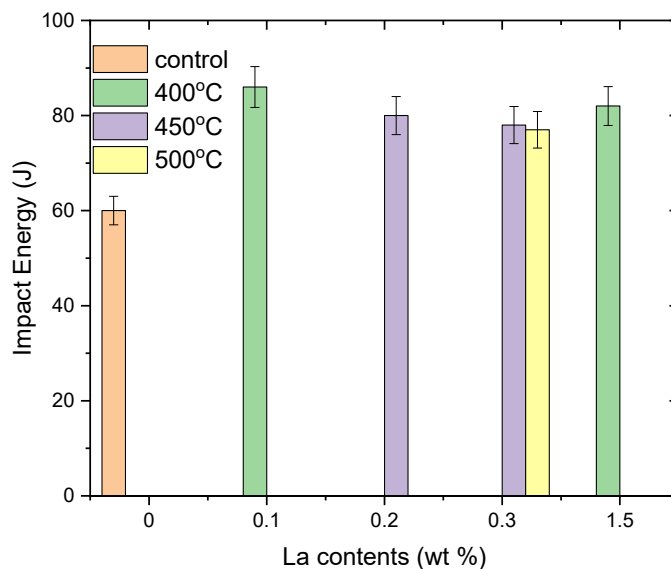


Fig. 3. Impact Energy of Cu-10Ni-xLa alloys at different ageing temperature.

3.3 Microstructural Evolution

The microstructural evolution induced by La additions and ageing at three temperatures was examined using optical microscopy (OM) and scanning electron microscopy (SEM). Figs 4 and 5 show micrographs illustrating the effects of La content and heat treatment on the morphology of the Cu-10Ni alloy. Both OM (Fig. 4) and SEM (Fig. 5) observations reveal a clear correlation between La content, ageing temperature, and microstructural refinement, confirming the role of La acts as an effective grain refiner and precipitation promoter. The as-cast control sample (Figs.4a and 5a) exhibits coarse dendritic and acicular (needle-like) phases. These structural features act as stress concentrators and adversely affect the alloy's properties (Zengin and Parvina, 2025). The addition of La at 0.1, 0.2, 0.3, and 1.5 wt.% followed by ageing treatments (Figs. 4b–e and 5b–e), transform the coarse dendritic matrix into finer, more coherent precipitates, indicating enhanced microstructural uniformity. Ageing at 400 °C and 450 °C results in a sparse distribution of fine precipitates along the grain boundaries (Zengin and Parvina, 2025 According to the Orowan strengthening mechanism, the finely distributed precipitates act as effective barriers to dislocation motion (Wang et al., 2023). These precipitates impede dislocation movement without inducing embrittlement, representing a classic case of controlled precipitation hardening (Cuniberti et al., 2010). In contrast, coarser precipitates enhance strength at the expense of ductility and toughness, which is consistent with the formation of a semi-continuous grain boundary phase. At an ageing temperature of 500 °C, the Cu-10Ni alloy containing 0.3 wt.% La (Figs. 4f and 5f) exhibits an over-aged microstructure. The optical micrographs reveal pronounced grain boundary thickening, while SEM observations show precipitates that have undergone significant coarsening and loss of coherence. This microstructural degradation leads to a reduction in tensile strength, hardness, and impact strength. The loss of precipitate coherence during over-ageing weakens the Orowan strengthening effect, thereby diminishing the overall mechanical performance of the alloy (Bai et al., 2024; Liu et al., 2025).

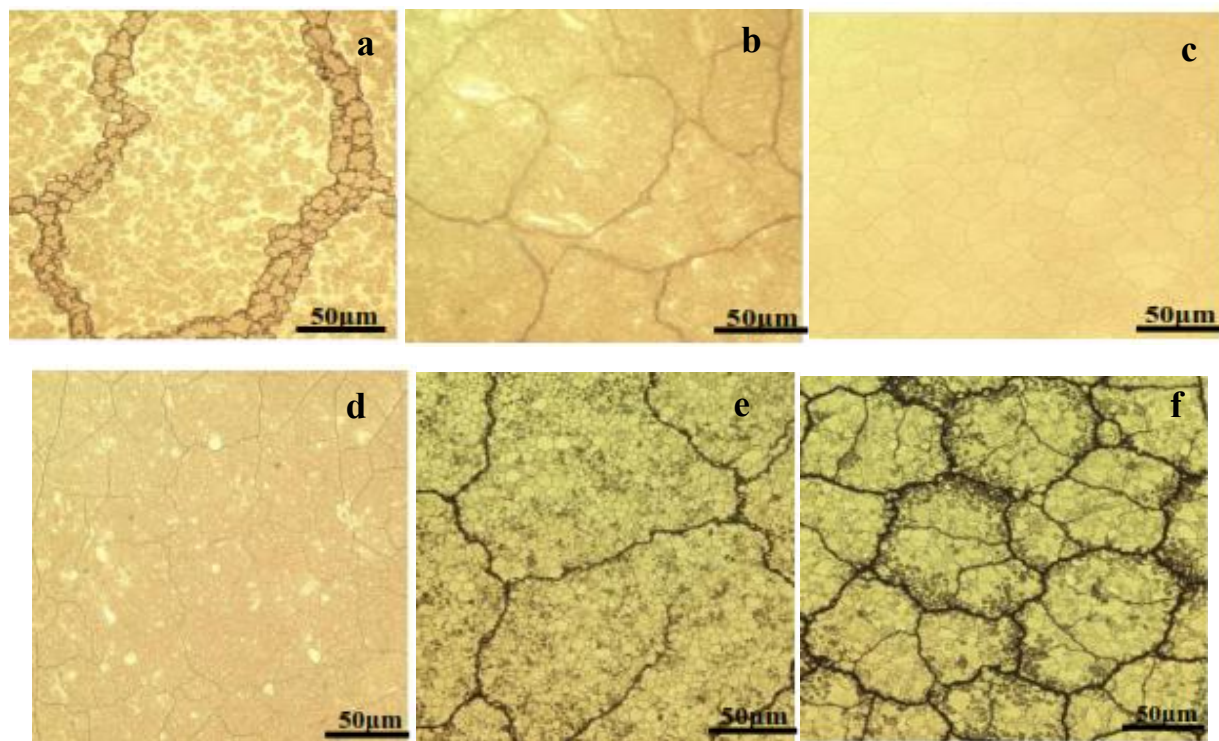


Fig. 4. Optical microstructure of Cu-10Ni-xLa (a) as-cast Cu-10Ni, (b) 0.1La/400 °C (c) 0.2La/450 °C (d) 0.3La/450 °C (e) 1.5La/400 °C (f) 0.3La/500 °C.

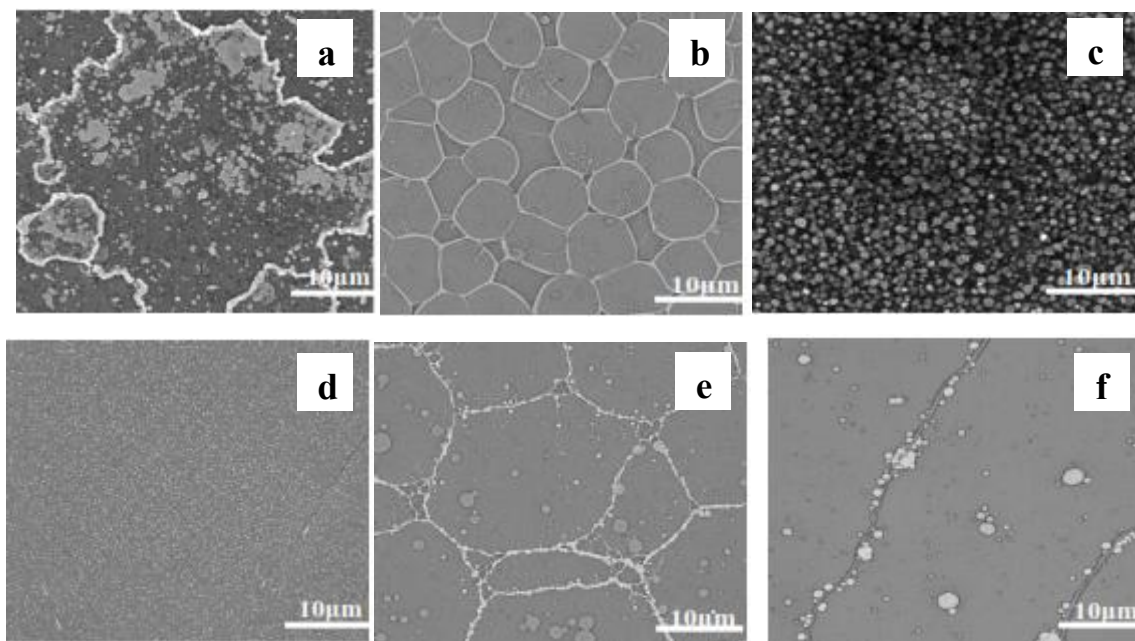


Fig. 5. SEM microstructure of Cu-10Ni-xLa (a) as-cast Cu-10Ni, (b) 0.1La/400 °C (c) 0.2La/450 °C (d) 0.3La/450 °C (e) 1.5La/400 °C (f) 0.3La/500 °C.

3.3.1 Microstructural Evolution and Structure–Property Correlation

Low-to-moderate lanthanum additions induced significant modifications in the microstructure and mechanical performance of the Cu-10Ni alloys. In line with established principles of rare-earth metallurgy, trace La additions (0.1–0.3 wt.%) promoted grain refinement,

grain boundary purification, and the controlled formation of nanoscale La-rich precipitates (Ji et al., 2018; Wang et al., 2023; Aliyu et al., 2024, Okechukwu et al., 2025). These microstructural features directly enhanced strength, hardness, toughness, and corrosion resistance, confirming La as an effective microalloying element for Cu-Ni systems within an optimal compositional range. At low La contents (0.1-0.3 wt.%), the combined effects of grain refinement and fine intragranular precipitation resulted in a substantial increase in strength without compromising ductility. The alloy aged at 450 °C with 0.3 wt.% La exhibited the most favourable microstructure, characterized by uniformly dispersed nanoscale precipitates, refined grains, and clean, impurity-free grain boundaries. This condition produced a synergistic strengthening effect through precipitation hardening, Orowan looping, and grain boundary strengthening, yielding a balanced property profile with high tensile strength (542 MPa), increased hardness (166.1 HBW), and improved toughness (78 J). Such balanced mechanical performance is characteristic of controlled rare-earth precipitation hardening, where coherent nanoparticles effectively hinder dislocation motion without acting as crack initiation sites (Hou, 2022; Semboshi et al., 2021). Ageing temperature played a critical role in precipitate evolution. Ageing at 400–450 °C favoured the nucleation of fine, thermally stable precipitates, enhancing strength while maintaining ductility. In contrast, increasing the ageing temperature to 500 °C promoted precipitate coarsening and loss of coherence, resulting in reduced tensile strength in the 0.3 wt.% La alloy. This over-ageing behaviour follows the classical kinetics of precipitation coarsening in copper alloys and is consistent with previous reports on Cu–RE systems (Aliyu et al., 2024; Semboshi et al., 2021). Moderate La additions (0.2 wt.%) aged at 450 °C further increased the tensile strength to 520 MPa; however, precipitate coarsening and the onset of grain boundary strengthening mechanisms led to reduced ductility and toughness. The formation of semi-continuous grain boundary phases is known to restrict grain boundary sliding and promote embrittlement, thereby explaining the observed reductions in elongation and impact energy (Wang et al., 2023; Semboshi et al., 2021). In contrast, a high La content (1.5 wt.%) resulted in excessive precipitation of coarse, brittle La-rich intermetallic compounds and the formation of continuous grain boundary networks. While this morphology increased hardness (154.2 HBW), it resulted in significant losses in ductility (21.58%), toughness (82 J), and corrosion resistance.

3.4 Electrochemical corrosion resistance

Figure 6a shows the Tafel polarization curves of Cu-10Ni alloys with varying La additions aged at different temperatures, while Figure 6b and **Table 3** summarize the corresponding electrochemical corrosion parameters. The corrosion behaviour is strongly influenced by both La content and ageing temperature, reflecting the underlying microstructural evolution. The base Cu-10Ni alloy exhibits a relatively high corrosion current density ($I_{\text{corr}} = 0.0612 \mu\text{A}\cdot\text{cm}^{-2}$) and a more negative corrosion potential ($E_{\text{corr}} = -0.6822 \text{ V}$), indicating comparatively poor corrosion resistance. This behaviour is attributed to its coarse dendritic microstructure and the presence of micro-galvanic sites that facilitate anodic dissolution (Ji et al., 2018; and Semboshi et al., 2021). With the addition of low-to-moderate La contents (0.1-0.3 wt.%) and appropriate ageing treatments, an improvement in corrosion resistance is observed. In particular, the alloy containing 0.2 wt.% La aged at 450 °C exhibits the lowest corrosion current density ($I_{\text{corr}} = 0.0406 \mu\text{A}\cdot\text{cm}^{-2}$) and the highest polarization resistance ($R_p = 1279 \Omega\cdot\text{cm}^2$), indicating superior corrosion resistance. This improvement is associated with refined grains, purified grain boundaries, and the uniform distribution of fine La-rich precipitates, which reduce active corrosion sites and promote the formation of a more stable and protective passive film. Also, the 0.3 wt.% La alloy aged at 450 °C shows a further reduction in corrosion current density ($I_{\text{corr}} = 0.0324 \mu\text{A}\cdot\text{cm}^{-2}$) and an increased polarization resistance ($R_p = 1603 \Omega\cdot\text{cm}^2$), confirming that controlled La additions enhance corrosion resistance by minimizing micro-galvanic coupling and improving surface film stability. Similar corrosion mitigation mechanisms induced by rare-earth elements have been reported by Wang et al. (2025) and Aliyu et al. (2024). The relatively positive shift in E_{corr} for these compositions also suggests a reduced thermodynamic tendency for corrosion (Semboshi et al., 2021; Nwaeju et al., 2022). Reduction in corrosion performance was observed with when 1.5 wt.% La was added to Cu-10Ni alloy, as evidenced by an increase in corrosion current density ($I_{\text{corr}} = 0.0869 \mu\text{A}\cdot\text{cm}^{-2}$) and a decrease in polarization resistance ($R_p = 597.96 \Omega\cdot\text{cm}^2$). This behaviour is attributed to the formation of coarse, brittle La-rich intermetallic phases and continuous grain boundary networks, which act as preferential corrosion initiation sites and disrupt the integrity of the passive layer. Furthermore, ageing at an elevated temperature of 500 °C (0.3 wt.% La) leads to increased corrosion current density ($I_{\text{corr}} = 0.1344 \mu\text{A}\cdot\text{cm}^{-2}$) and reduced polarization resistance ($R_p = 386.89 \Omega\cdot\text{cm}^2$), indicating reduced corrosion resistance. This degradation is consistent with precipitate coarsening and grain boundary thickening associated with over-ageing, which enhance localized corrosion susceptibility as reported for Cu–RE systems by Semboshi et al. (2021) and Bai et al. (2024). Overall, the electrochemical results demonstrate that optimal La additions (0.2-0.3 wt.%) combined with ageing at 400-450 °C significantly enhance corrosion resistance, whereas excessive La content or over-ageing conditions adversely affect electrochemical stability. These trends closely correlate with the observed microstructural refinement and structure–property relationships discussed by previous authors.

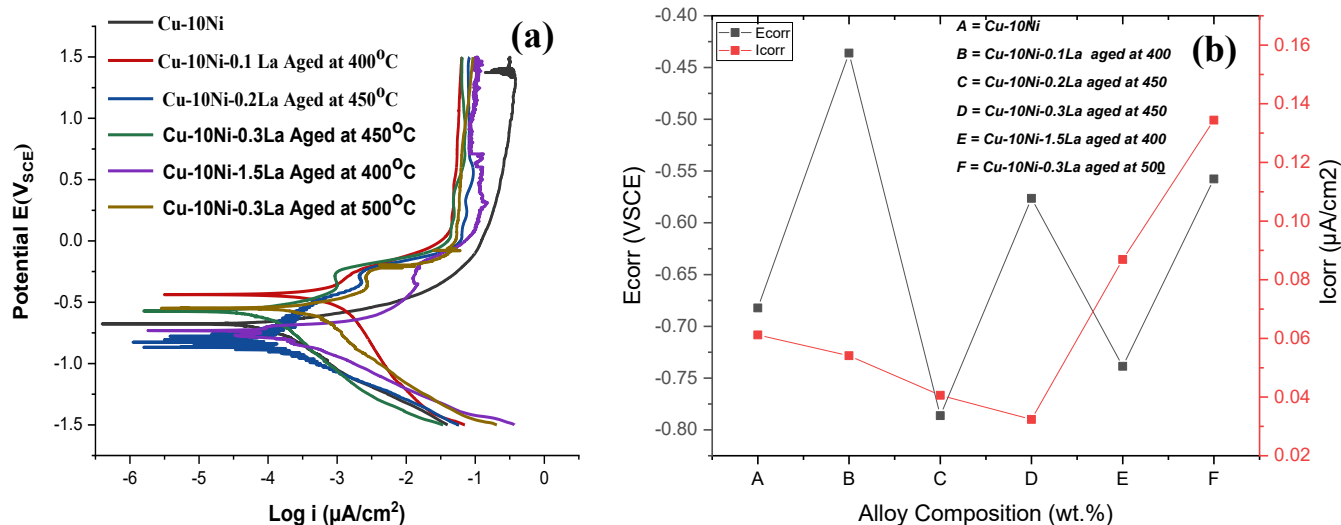


Fig. 6. (a) Tafel curves (b) Electrochemical corrosion characteristics of Cu-10Ni alloy with varying La additions at different ageing temperature.

Table 2. Electrochemical polarization parameters of Cu-10Ni alloy with varying La additions at different ageing temperature

Alloy Composition (wt.%)	Ageing Temperature (°C)	Electrochemical Parameters Associated with Polarization Measurement						
		I_{corr} ($\mu A/cm^2$)	E_{corr} (V _{SCE})	R_p (Ωcm^2)	β_c (V.dec ⁻¹)	β_a (V.dec ⁻¹)	Corri (A)	CR (mm/yr)
Cu-10Ni	0	0.0612	-0.6822	849.02	5.771	11.528	1.172	0.229
Cu-10Ni-0.1La	400	0.0541	-0.4361	1173	4.285	3.463	6.588	0.214
Cu-10Ni-0.2La	450	0.0406	-0.7863	1279	7.487	8.03	8.67	0.169
Cu-10Ni-0.3La	450	0.0324	-0.5764	1603	4.040	7.435	9.35	0.182
Cu-10Ni-1.5La	400	0.0869	-0.7386	597.96	4.242	10.984	1.891	0.369
Cu-10Ni-0.3La	500	0.1344	-0.5577	386.89	3.064	6.942	4.449	0.867

3.5 ANFIS Modelling and Optimisation of Al-Cu-La

The predictive capability of the developed ANFIS model was first evaluated using training performance metrics, namely the root mean square error (RMSE) and coefficient of determination (R^2), for all investigated properties as given in Table 4. The results indicated strong agreement between experimental and predicted values, with R^2 ranging from 0.958 to 0.972 and correspondingly low RMSE values for ultimate tensile strength (4.37 MPa), hardness (3.12 HBW), impact toughness (2.85 J), and corrosion current density (0.0023 $\mu A/cm^2$). These high R^2 values (>0.95) demonstrate that the ANFIS model accurately captured the nonlinear relationships between lanthanum content, ageing temperature, and the mechanical and corrosion properties of the developed Al-Cu matrix composite. The low prediction errors further confirm the robustness and generalisation capability of the trained model.

Table 4. Training Performance Results

Output	Training RMSE	R^2 (Training)
UTS (MPa)	4.37	0.972
Hardness (HBW)	3.12	0.964
Impact Toughness (J)	2.85	0.968
Corrosion Current Density ($\mu A/cm^2$)	0.0023	0.958

On the basis of this high predictive accuracy, the trained ANFIS model was subsequently employed for multi-objective optimisation using a desirability function approach to simultaneously maximise strength, hardness, and toughness while minimising corrosion current density. The output of the analysis was presented in **Table 5**. The optimisation identified 0.20 wt.% lanthanum addition and an ageing temperature of 450 °C as the optimal parameter combination, yielding predicted ultimate tensile strength of 518–522 MPa, hardness of 182–186 HBW, impact toughness of 78–82 J, and corrosion current density of 0.039–0.042 $\mu\text{A}/\text{cm}^2$. The desirability index obtained ($D = 0.94$) is close to unity, indicating that the selected processing conditions provide a near-ideal compromise among all targeted properties. The reliability of the optimised solution is directly supported by the strong training performance of the ANFIS model. For example, the RMSE associated with UTS prediction (4.37 MPa) is very small relative to the optimised strength level (~ 520 MPa), while the hardness and toughness errors (≈ 3 HBW and ≈ 3 J) are similarly negligible compared with their predicted magnitudes. Even for corrosion current density, which typically exhibits higher experimental variability, the RMSE (0.0023 $\mu\text{A}/\text{cm}^2$) remains extremely small relative to the optimised value (~ 0.04 $\mu\text{A}/\text{cm}^2$). These low relative errors confirm that the predicted optimum properties fall well within the reliable prediction domain of the trained ANFIS model.

Table 5. Optimized Solution Identified by ANFIS

Parameter	Optimized Value
Lanthanum Content	0.20 wt.%
Ageing Temperature	450 °C
Predicted UTS	518–522 MPa
Predicted Hardness	182–186 HBW
Predicted Toughness	78–82 J
Predicted Corrosion Current Density	0.039–0.042 $\mu\text{A}/\text{cm}^2$
Desirability Index (D)	0.94

3.6 Influence on Alloy Selection

Aligning the model data with the experimental results, the predicted optimum at 0.20 wt.% La and 450 °C ageing temperature corresponds to peak precipitation-hardening conditions combined with effective rare-earth-induced microstructural refinement. At this lanthanum level, grain refinement and intermetallic dispersion strengthening are maximised without excessive formation of brittle phases, thereby enabling simultaneous improvement in strength and toughness. The elevated ageing temperature promotes the formation of fine, uniformly distributed θ' (Al_2Cu) precipitates, which enhance base strengthening and hardness while maintaining adequate ductility (Wang et al., 2023). Furthermore, the refined and homogenised microstructure reduces micro-galvanic coupling sites, leading to the observed reduction in corrosion current density. Overall, the close agreement between experimental data and ANFIS predictions, together with the high desirability index of the optimised solution, confirms that the developed ANFIS-based framework is an effective tool for modelling and optimisation of processing–composition–property relationships in Cu-Ni alloy doped with lanthanum.

4. Conclusions

1. The influence of lanthanum (La) microalloying and ageing treatment on the microstructure, mechanical properties, and corrosion behaviour of Cu–10Ni alloys has been investigated. The results show that both La content and ageing temperature play a critical role in controlling microstructural evolution and overall alloy performance.
2. Low-to-moderate La additions (0.1–0.3 wt.%) led to significant grain refinement, grain boundary purification, and the formation of fine, uniformly distributed La-rich precipitates. These microstructural modifications resulted in notable improvements in tensile strength, hardness, toughness, and corrosion resistance. The alloy containing 0.2 wt.% La aged at 450 °C exhibited the most balanced combination of properties due to the combined effects of grain refinement and precipitation strengthening.
3. Ageing at 400–450 °C promoted the formation of fine, coherent precipitates, enhancing strength while maintaining ductility and electrochemical stability. In contrast, ageing at 500 °C caused precipitate coarsening and over-ageing, leading to reduced mechanical strength and corrosion resistance.
4. Moderate La additions (0.2–0.3 wt.%) give the optimal balance of strength, toughness and corrosion resistance due to precipitate coarsening and the development of grain boundary phases. Higher La addition (≥ 1.5 wt.%) was found to degrade overall alloy

performance. Despite modest hardness enhancements (154.2 HBW), the formation of brittle La-rich intermetallic compounds, resulted in significant losses in ductility (21.58%) and corrosion resistance, confirming that rare-earth additions beyond the optimal range compromise property balance.

5. The combined experimental and ANFIS optimization results confirmed that controlled La microalloying in the range of 0.2 - 0.3 wt.% combined with ageing at is 450 °C gives the most favourable compromise between strength, toughness and corrosion resistance. This composition and ageing conditions provide the optimal design strategy for high-performance Cu-Ni alloys.

Credit Author Contribution Statement

A. B. Okoubulu: Conceptualization, Writing – Original Draft, Project Administration

C. C. Nwaeju-Okechukwu: Investigation, Data Curation, supervision

A. B. Okoubulu and C. C. Nwaeju-Okechukwu: Methodology, Validation

Declaration Statements

Funding

This research received no external funding.

Conflicts of Interest

The authors declare that they have no known financial or competing interests that could have appeared to influence the work reported in this paper.

Nomenclature

Symbol	Description	Unit
I_{corr}	Corrosion density	$\mu A/cm^2$
E_{corr}	Corrosion potential	V_{SCE}
β_c	cathodic tafel slope	$V.dec^{-1}$
β_a	anodic tafel slope	$V.dec^{-1}$
CR	Corrosion rate	mm/yr
R_p	Linear polarization resistance	Ωcm^2
Corr i	Corrosion current	A

References

- Aliyu, S. J., Adekanye, T., Adediran, A. A., & Ogundipe, O. (2025). Influence of micro-addition of lanthanum on grain characteristics, mechanical properties, and corrosion behavior of CuAlNiMnLa shape memory alloy, *Research on Engineering Structures & Materials*, 11(3), 1-17. <http://dx.doi.org/10.17515/resm2024.347me0710rs>
- Bai, Y., Zheng, S., Liu, N., Liu, Y., Wang, X., Qiu, L., & Gong, A. (2024). The Role of Rare Earths on Steel and Rare Earth Steel Corrosion Mechanism of Research Progress. *Coatings*, 14(4), 465. <https://doi.org/10.3390/coatings14040465>
- Cuniberti, A., Tolley, A., Riglos, M. C., & Giovachini, R. (2010). Influence of natural aging on the precipitation hardening of an AlMgSi alloy. *Materials Science and Engineering: A*, 527(20), 5307-5311. <https://doi.org/10.1016/j.msea.2010.05.003>
- Gao, H., Guan, K., Cui, R. J., Qin, J. C., Zhao, Z. H., & Huang, Z. H. (2025). Effect of lanthanum on microstructure of a nickel-based single crystal superalloy. *China Foundry*, 22(1), 55-64. <https://doi.org/10.1007/s41230-025-4006-4>.
- Guo, C., Kang, T., Wu, S., Ying, M., Liu, W. M., & Chen, F. (2021). Microstructure, mechanical, and corrosion resistance of copper nickel alloy fabricated by wire-arc additive manufacturing. *MRS Communications*, 11(6), 910-916. <https://doi.org/10.1557/s43579-021-00120-1>
- Hou, J. X., Cao, B. X., Xiao, B., Jiao, Z. B., & Yang, T. (2022). Compositionally complex coherent precipitation-strengthened high-entropy alloys: a critical review. *Rare Metals*, 41(6), 2002-2015. <https://doi.org/10.1007/s12598-021-01953-4>.

- Hou, R., Wu, M., Li, Q., Li, W., Chen, D. L., & Li, D. Y. (2021). Effects of Mo and B additives on hardness and the resistance of Cu–Ni alloy to wear, corrosion and corrosive wear. *Metals and Materials International*, 27(12), 4911–4921. <https://doi.org/10.1007/s12540-020-00801-x>
- Ji, Y., Zhang, M.-X., & Ren, H. (2018). Roles of Lanthanum and Cerium in Grain Refinement of Steels during Solidification. *Metals*, 8(11), 884. <https://doi.org/10.3390/met8110884>
- Jing, F., Liu, Y., Yang, B., Shi, C., Du, Y., & Zhang, L. (2026). Study on microstructure and properties of Cu–Cr–Zr–Mg alloy with various Y contents and aging parameters. *Journal of Alloys and Compounds*, 185995. <https://doi.org/10.1016/j.jallcom.2026.185995>
- Krupińska, B., Rdzawski, Z., Krupiński, M., & Pakielna, W. (2020). Precipitation Strengthening of Cu–Ni–Si Alloy. *Materials*, 13(5), 1182. <https://doi.org/10.3390/ma13051182>
- Lian, X. T., Chen, L., Fan, Z. W., Liu, T. S., Xu, D. X., & Dong, H. (2022). Effects of modified inclusions and precipitates alloyed by rare earth element on corrosion and impact properties in low alloy steel. *Acta Metallurgica Sinica (English Letters)*, 35(10), 1719–1730. <https://doi.org/10.1007/s40195-022-01404-8>
- Lian, X., Zhao, H., Chen, L., Liu, T., Feng, Q., Li, H., Shi, Y., & Dong, H. (2023). Effects of Rare Earth Elements on Microstructure and Corrosion Resistance of Low Alloy Steel Based on Ultra-Thin Cast Strip Process. *Metals*, 13(1), 66. <https://doi.org/10.3390/met13010066>
- Liu, J. S., Yu, W. X., Chen, D. Y., Wang, S. W., Song, H. W., & Zhang, S. H. (2025). A review of studies on the influence of rare-earth elements on the microstructures and properties of copper and copper alloys and relevant applications. *Metals*, 15(5), 536. <https://doi.org/10.3390/met15050536>
- Mahmoud, M. G., Zedan, Y., Samuel, A. M., Doty, H. W., Songmene, V., & Samuel, F. H. (2022). Effect of rare earth metals (Ce and La) addition on the performance of Al–Si–Cu–Mg cast alloys. *International Journal of Metalcasting*, 16(3), 1164–1190. <https://doi.org/10.1007/s40962-021-00669-6>
- Nwaeju, C. C., Eboh, A. O., & Edoziuno, F. O. (2022). Research Paper Grain Size Evolution, Mechanical and Corrosion Behaviour of Precipitate Strengthened Cu–Ni Alloy. *Acta Metallurgica Slovaca*, 28(4), 188–196. <https://doi.org/10.36547/ams.28.4.1609>
- Nwaeju, C. C., Edoziuno, F. O., Adediran, A. A., Nnuka, E. E., & Adesina, O. S. (2021). Structural and properties evolution of copper–nickel (Cu–Ni) alloys: a review of the effects of alloying materials. *Matériaux & Techniques*, 109(2), 204. <https://doi.org/10.1051/mattech/2021022>
- Nwaeju-Okechukwu, C. C., Okuma, S. O., Abd El-Rehim, A. F., Zahran, H. Y., & Edoziuno, F. O. (2025). Optimization of physical and hardness properties of epoxy composites reinforced with Meretrix lusoria Shell particulates using RSM. *Results in Chemistry*, 102771. <https://doi.org/10.1016/j.rechem.2025.102771>
- Okechukwu, C. C., Edoziuno, F. O., Adediran, A. A., Okuma, S. O., & Okoubulu, A. B. (2025). Experimental and process modelling of chemical composition and thermal ageing of Ti-doped cast Cu–Ni alloy for microstructural, conductivity, and mechanical properties. *Journal of Alloys and Metallurgical Systems*, 9, 100141. <https://doi.org/10.1016/j.jalms.2024.100141>
- Peng, C.-H., Hou, P.-Y., Lin, W.-S., Shen, P.-K., Huang, H.-H., Yeh, J.-W., Yen, H.-W., Huang, C.-Y., & Tsai, C.-W. (2023). Investigation of Microstructure and Wear Properties of Precipitates-Strengthened Cu–Ni–Si–Fe Alloy. *Materials*, 16(3), 1193. <https://doi.org/10.3390/ma16031193>
- Semboshi, S., Hariki, R., Shuto, T., Hyodo, H., Kaneno, Y., & Masahashi, N. (2021). Age-induced precipitating and strengthening behaviors in a Cu–Ni–Al alloy. *Metallurgical and Materials Transactions A*, 52(11), 4934–4945. <https://doi.org/10.1007/s11661-021-06435-x>
- Shi, Y. F., Guo, C. J., Yuan, M. Q., Jia, Z. B., An, G. H., Xiao, X. P., & Yang, B. (2023). Effect of solidification rate on dendrite segregation and mechanical properties of Cu–15Ni–8Sn alloy prepared by directional solidification: YF Shi et al. *Journal of Iron and Steel Research International*, 30(8), 1586–1597. <https://doi.org/10.1007/s42243-023-01015-2>
- Wang, M., Chen, S., Wang, S., Zhang, M., Song, H., & Zhang, S. (2023). Effects of La addition on microstructure evolution and thermal stability of Cu–2.35 Ni–0.59 Si sheet. *Materials*, 16(11), 4105. <https://doi.org/10.3390/ma16114105>
- Wang, XY., Liu, WF., Dong, X., Li, N., Zheng, Y. & Zhao, H. (2025) The effect of Rare Earth (RE) elements on corrosion and mechanical properties of Magnesium (Mg) alloys: a review. *Physica Scripta*. <https://doi.org/10.1088/1402-4896/adb081>
- Wu, D., Hu, J., Hu, Q., Wu, L., Guan, B., Zeng, S., Xing, Z., Wang, J., Xu, J., Huang, G., & Liu, J. (2025). The Effect of Aging Treatment on the Properties of Cold-Rolled Cu–Ni–Si–Co Alloys with Different Mg Contents. *Materials*, 18(14), 3263. <https://doi.org/10.3390/ma18143263>
- Yu, Q., Zhang, L., Zhang, Y., Chen, Y., Wang, S., & Yu, H. (2025). Effect of La on Microstructure and Corrosion Resistance of Oxygen-Free Copper Heat Tubes. *The Journal of The Minerals, Metals & Materials Society (TMS)*, 1–9. <https://doi.org/10.1007/s11837-025-07844-8>

- Zengin, E., & Irgasheva, P. (2025). Influence of Mg, Sr, TiB, and Cu Additions on the Microstructure and Mechanical Behavior of A356 Alloy Wheels. *Journal of Advanced Applied Sciences*, 4(1-2), 37-44.. <https://doi.org/10.61326/jaasci.v4i1-2.420>
- Zhang, M., Yang, J., Huang, C., Ying, P., Huan, Y., & Liu, F. (2024). Effect of Microalloying Rare-Earth Nd on Microstructure Evolution and Mechanical Property of Cu Alloy. *Materials*, 17(20), 5112. <https://doi.org/10.3390/ma17205112>
- Zhou, F., Zhou, Y., Song, K., Zhang, Y., Yang, R., Yang, S., Lu, L., Yu, Y., Liu, L., Chen, J., Jiang, K., & Yang, W. (2024). The influence of microalloying and preparation process on phase transformation, mechanical properties, and friction/corrosion behavior of Cu–Ni–Sn alloys: A review. *Journal of Materials Research and Technology*, 28, 951-966. <https://doi.org/10.1016/j.jmrt.2023.12.073>